NUCLEAR SCIENCE AND TECHNIQUES **25**, 060602 (2014)

The performance of Pt/air oxygen sensors in stagnant Pb-Bi eutectic at high temperatures*

WANG Yan-Qing (王艳青),[1,2] HUANG Qun-Ying (黄群英),[1,2] WU Bin (吴斌),[2,†]
ZHANG Min (张敏),[1,2] WU Xin (武欣),[2] and GAO Sheng (高胜)[2]

[1] *University of Science and Technology of China, Hefei 230027, China*
[2] *Institute of Nuclear Energy Safety Technology, Chinese Academy of Sciences, Hefei 230031, China*

(Received January 22, 2014; accepted in revised form March 18, 2014; published online December 16, 2014)

Oxygen control technology is a critical issue for compatibility of candidate structural materials with liquid lead-bismuth eutectic (LBE) in accelerator driven systems. Performances of a self-developed Pt/air sensor and another one from Karlsruher Institute of Technology (KIT) were tested in stagnant oxygen-saturated liquid LBE. Calibrations showed that the trend and values of corrected electromotive force (EMF) of the self-developed sensor, with a bias voltage of 20 mV, were consistent with theoretical results above 425 °C, and similar results were obtained in cross-calibration test with EMF value of KIT sensor as reference. In stability test at 450 °C for 100 hours, the KIT sensor performed better than the self-developed one, which showed signal fluctuations. Both sensors exhibited quick response to temperature variations in the responsiveness test.

Keywords: Lead-bismuth eutectic, Oxygen sensor, Calibration, Electromotive force

DOI: 10.13538/j.1001-8042/nst.25.060602

I. INTRODUCTION

Driven by the need of candidate materials for spallation neutron target and coolant in accelerator driven systems (ADS), lead-bismuth eutectic (LBE) has been studied widely due to its good thermal-physical and chemical properties. However, liquid LBE is corrosive to structural material at high temperatures and may cause plugging due to the formation of lead monoxide (PbO). For compatibility of the materials with LBE, oxygen contents in LBE should be kept in certain margin to form protective oxide films on surface of the structural materials and to prevent the formation of PbO [1–7].

As accurate oxygen content measurement is a prerequisite for oxygen control technology, oxygen sensor plays a critical role in an active oxygen control system (OCS). In the lead or LBE system, yttria-stabilized zirconia (YSZ) or magnesia-stabilized zirconia (MSZ) are employed as solid electrolyte for oxygen sensors [8], and YSZ is more widely used [1, 3, 9]. It is generally accepted that Russian scientists paved the way to the development of oxygen sensor and oxygen control technology [6, 8]. The oxygen sensors developed in Russia are accurate in measuring oxygen content, with long service lifetime [10]. Oxygen sensors have been studied widely. Konys *et al*. found that oxygen sensors with Pt/air reference electrode showed better reliability and longer lifetime than those with Bi/Bi_2O_3 reference electrode, from the tests carried out in the CORRIDA loop and other devices in Karlsruher Institute of Technology (KIT) [2, 11]. Courouau *et al*. developed the oxygen sensor with Bi/Bi_2O_3 reference electrode [3, 12, 13]. Kurata *et al*. studied Pt/air and Bi/Bi_2O_3 reference sensors and found electromotive force (EMF) values of both sensors could be corrected by subtracting certain bias voltage, though physics meaning of the bias voltage was not quite clear [8]. It is necessary to check the performance of a newly assembled oxygen sensor before its use in liquid LBE system, for its high accuracy, reproducibility, long-term stability and short response time [14].

Having been working on heavy liquid metal (HLM) technologies for over ten years [15–21], the FDS team is now studying on key technologies of liquid LBE loops named KYLIN series, focusing on corrosion of the materials, thermal-hydraulics, oxygen measurement and control, and so on [22–24]. For oxygen measurement, two Pt/air sensors, the self-developed Sensor 1 and Sensor 2 from KIT, were tested in oxygen-saturated liquid LBE. The accuracy of Sensor 1 was calculated and cross-calibrated with the EMF values of Sensor 2. The stability and responsiveness of both sensors were tested, too.

II. METHODS

A. The oxygen sensor

Electrochemical oxygen sensors are based on the EMF measurement method at null current for a galvanic cell built with a doped zirconia solid electrolyte, which conducts specifically oxygen ions [25]. A Pt/air reference oxygen sensor with YSZ as solid electrolyte is illustrated schematically in Fig. 1 [9, 24, 26]. The oxygen partial pressure in the reference electrode ($p_{O_2,ref}$) is higher than the partial pressure of dissolved oxygen in LBE (p_{O_2}). The oxygen ions (O^{2-}) move through the solid electrolyte toward the LBE side, and electrons are transferred back to the reference side through the connecting wires, hence the formation of EMF across the solid electrolyte, which can be measured by a high impedance electrometer [25, 27] with impedance $> 1\,G\Omega$ in general [1].

* Supported by the National Nature Science Foundation of China (No. 51301163) and the Important Direction Program of Chinese Academy of Sciences (No. XDA03040200)
† Corresponding author, bin.wu1@fds.org.cn

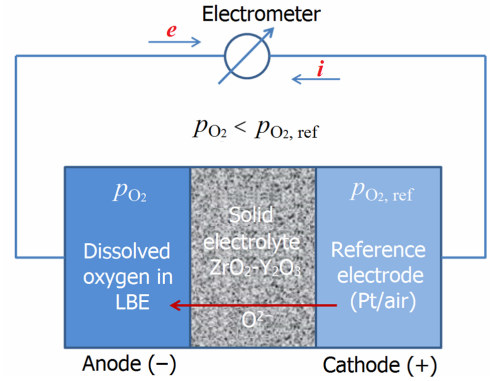

Fig. 1. (Color online) Schematic illustration of Pt/air oxygen sensor.

The cell can be expressed as the following form [27]

$$(-)\mathrm{SS}|\mathrm{Pb},\mathrm{PbO}|\mathrm{YSZ}|\mathrm{Pt},\mathrm{O_2}|\mathrm{SS}(+). \tag{1}$$

The left side is the oxidation process

$$\mathrm{Pb} + \mathrm{O_2^-} \rightarrow \mathrm{PbO} + 2\mathrm{e^-}. \tag{2}$$

The right side is the reduction process

$$\mathrm{O_2(g)}/2 + 2\mathrm{e^-} \rightarrow \mathrm{O_2^-}. \tag{3}$$

The total reaction is

$$\mathrm{Pb} + \mathrm{O_2(g)}/2 \rightarrow \mathrm{PbO}. \tag{4}$$

B. EMF of oxygen sensor

According to the Nernst equation, the EMF value of oxygen sensor is expressed as [6]:

$$E = (RT/4F)\ln(p_{\mathrm{O_2,ref}}/p_{\mathrm{O_2}}), \tag{5}$$

where E is in V and T is in K (being so throughout the text), $R = 8.314\,51$ J/(mol K) is the perfect gas constant, and $F = 96\,485.31$ C/mol is the Faraday constant. The $p_{\mathrm{O_2,ref}}$ is given at a certain temperature, and the $p_{\mathrm{O_2}}$ can be calculated by Eq. (5). It is valid by assuming that the solid electrolyte is of pure ionic conduction, and that all transfers at interfaces developed in the electrochemical cell are reversible [6, 9].

Inserting the values of R and F into Eq. (5) yields, one has:

$$E = 2.1543 \times 10^{-5} T \ln(p_{\mathrm{O_2,ref}}/p_{\mathrm{O_2}}). \tag{6}$$

For Pt/air sensors, the reference oxygen partial pressure is determined by the volume concentration of oxygen in air (with 20.946 vol% in general), then

$$p_{\mathrm{O_2,ref}}/p^{\ominus} = 0.20946, \tag{7}$$

where $p^{\ominus}$ is the standard atmospheric pressure. Inserting Eq. (7) into Eq. (6), one has

$$E = [-3.3677 - 2.1543\ln(p_{\mathrm{O_2}}/p^{\ominus})] \times 10^{-5} T. \tag{8}$$

The oxygen partial pressure above the saturated LBE, $p_{\mathrm{O_2,s}}$, and the oxygen partial pressure above the unsaturated solutions, $p_{\mathrm{O_2}}$, can be calculated by Eqs. (9) and (10) [28]:

$$p_{\mathrm{O_2,s}}/p^{\ominus} = \exp[25.624 - (52341/T)], \tag{9}$$

$$p_{\mathrm{O_2}}/p^{\ominus} = C_{\mathrm{O}}^2 \exp[13.558 - (32005/T)], \tag{10}$$

where C_{O} is the oxygen concentration in wt%. Inserting Eqs. (9) and (10) into Eq. (8), respectively, one has [28]

$$E_{\mathrm{th}} = 1.1276 - 5.8568 \times 10^{-4} T, \tag{11}$$

$$\log C_{\mathrm{O}} = -3.2837 - (6949.8\text{–}10080E)/T, \tag{12}$$

where E_{th} is the theoretical EMF for oxygen saturated LBE.

C. Experimental apparatus and procedures

Figure 2 shows the schematics and photo of the experimental apparatus. It consists mainly of a gas control system, an experimental tank with three positions for installing oxygen sensors, and a data acquisition (DAQ) system.

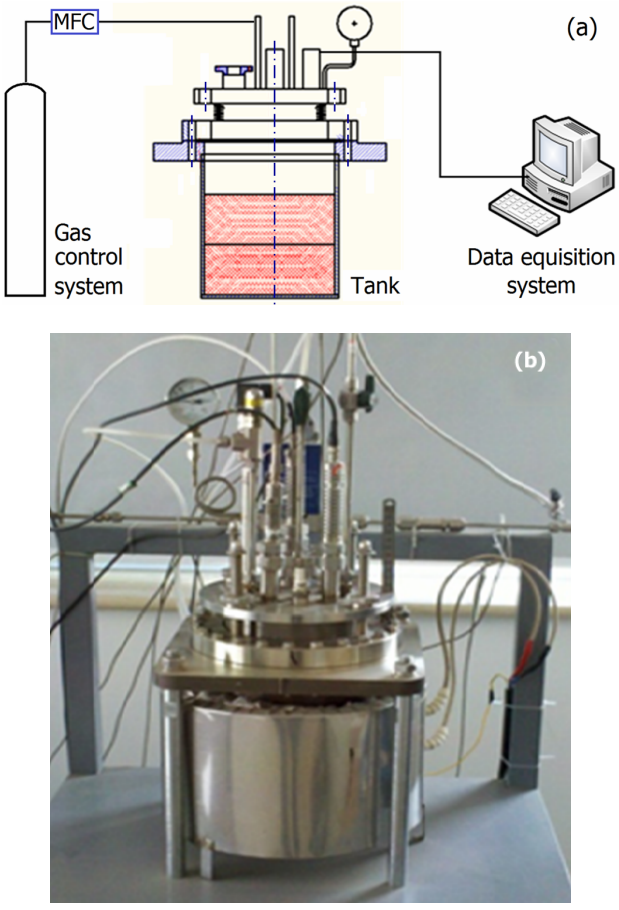

Fig. 2. (Color online) The experimental apparatus.

Oxygen sensors were mounted onto the tank (Fig. 2(b)), air tightness of the tank was checked, and the LBE was melted. Then, the oxygen sensors were inserted about 30 mm into the liquid LBE by depressing the bellows. EMF values of the oxygen sensors and temperature of LBE were recorded by the DAQ system with LabVIEW.

The Ar+2%O_2 gas mixture in a flow rate of 10 mL/min in was introduced continually into the tank as cover gas, and the oxygen partial pressure of this mixed gas was higher than the oxygen pressure for PbO formation in liquid LBE [29], therefore the liquid LBE was saturated with oxygen.

III. RESULTS AND DISCUSSION

A. Calibration

An oxygen sensor should be calibrated so as to check if its EMF output is accurate [9]. The calibration was carried out in oxygen-saturated LBE at 370–540 °C [25]. As shown in Fig. 3, the measured EMF data of Sensor 1 (E_{S1}) were lower than the theoretical prediction ($E_{th,\,oxygen\text{-}saturated}$) [28], but it can be seen that above 425 °C the E_{S1} variation trend is consistent with the E_{th}, indicating that Sensor 1 did not work reliably below 425 °C. Similar results were reported [6, 8]. This was caused by insufficient diffusion rate of oxygen ions in solid electrolyte at low temperatures [30], which increases irreversibility of the cell, and thus Eq. (5) is no longer suitable to the cell [6]. For LBE in oxygen-saturated condition, a bias voltage can be considered [8]. The bias voltage was 20 mV at above 425 °C and the E_{S1} were measured again. Fig. 3 shows, the corrected EMF data of Sensor 1 ($E_{S1\text{-}corrected}$) agree well with the E_{th} above 425 °C. The deviation of E_{S1} can be related to the electrolyte conduction properties, alteration of electrode/electrolyte interface, and resistant of the Pt/air electrode. Sensor 1 was cross-calibrated with Sensor 2, which has been calibrated at KIT and is a suitable reference. Fig. 3 shows also the EMF data of Sensor 2 (E_{S2}) and $E_{S1\text{-}corrected}$. They are consistent with each other above 425 °C, being similar to the results using E_{th} as reference.

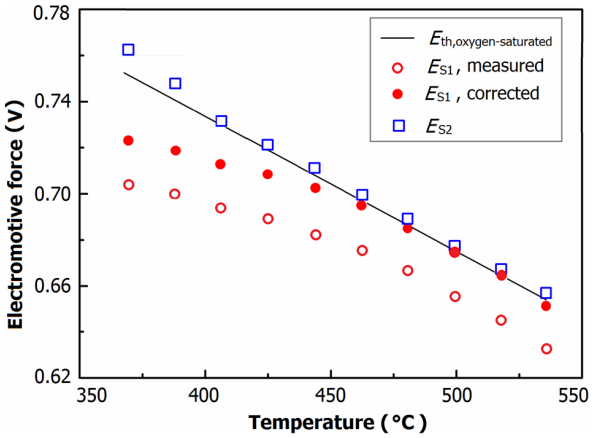

Fig. 3. (Color online) EMF of Sensor 1 as function of the temperature, calibrated with theoretical EMF and EMF of Sensor 2.

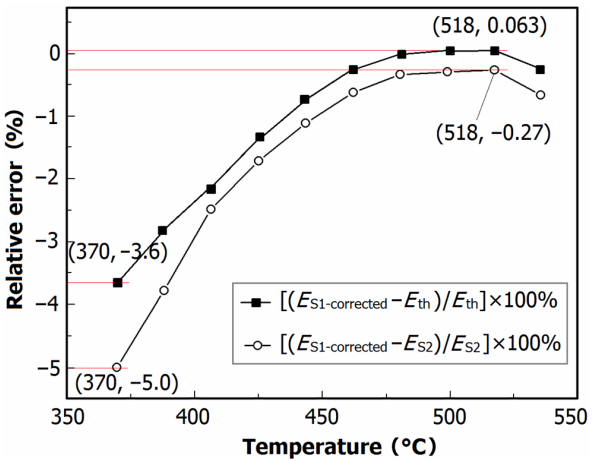

Fig. 4. (Color online) The relative error of $E_{S1\text{-}corrected}$ with E_{th} and E_{S2}, as function of temperature.

The relative errors of $E_{S1\text{-}corrected}$ are shown in Fig. 4. Referenced by E_{th} and E_{S2}, the maximum and minimum were −3.6% at 370 °C and 0.063% at 518 °C, and −5.0% at 370 °C and −0.27% at 518 °C, respectively. Therefore, the accuracy of $E_{S1\text{-}corrected}$ is assessed within ±5% of the relative error.

Based on the results, Sensor 1 (with a bias voltage of 20 mV) was suitable to measure dissolved oxygen concentration (C_O) in LBE above 425 °C, and the corresponding oxygen concentrations calculated with Eq. (12) [29] confirmed the points hereinbefore (Fig. 5). The oxygen concentrations calculated with $E_{S1\text{-}corrected}$ ($C_{O,S1\text{-}corrected}$) and E_{S2} ($C_{O,S2}$) as input variables are consistent with the theoretical saturated oxygen contents ($C_{O,oxygen\text{-}saturated}$) calculated with EMF from Eq. (11) as input variables.

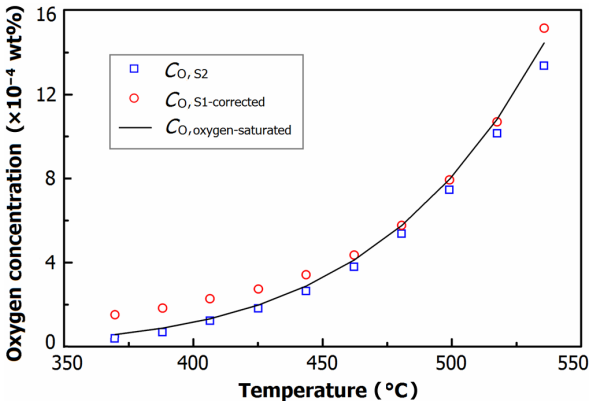

Fig. 5. (Color online) Oxygen contents in oxygen-saturated LBE, as function of temperature, calculated using $E_{S1\text{-}corrected}$, E_{S2} and E_{th}.

B. Stability test

Checking the stability of an oxygen sensor under certain condition is essential to actual use [12, 31]. Stability test of Sensors 1 and 2 was carried out in stagnant oxygen-saturated

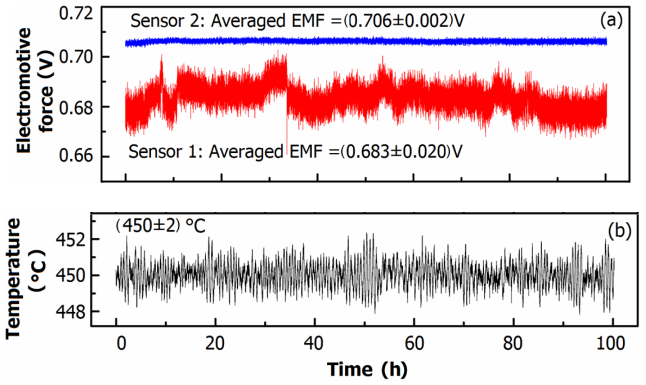

Fig. 6. (Color online) Stability test of Sensors 1 and 2 at 450 °C: EMF(a) and temperature (b) fluctuations in 100 h.

LBE at 450 °C for 100 h. As shown in Fig. 6, the Averaged EMF was (0.683 ± 0.020) V and (0.706 ± 0.002) V, for Sensors 1 and 2, respectively, while the calculated EMF was 0.704 V at 450 °C. The temperature fluctuation during the 100 h was ±2 °C (Fig. 6(b)).

The results show that Sensor 2 performed nicely in the test, comparing the experimental and theoretical EMF values [31]. For Sensor 1, large fluctuations were seen during the 100 hours; with a bias voltage of 20 mV, however, the mean EMF value (0.703 V) agrees well with the theoretical value of 0.704 V.

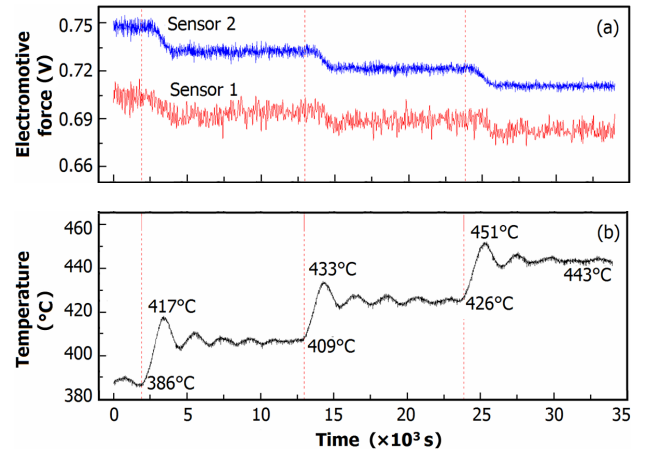

Fig. 7. (Color online) EMF response of Sensors 1 and 2 as function of temperature.

C. Responsiveness test

Response time to changes in operation conditions is important for oxygen sensors used in LBE [14, 25]. Fig. 7 shows the response test results of Sensors 1 and 2 with three stages of heating (see the dashed line in the figure), both sensors exhibited fast response (Fig. 7(a)), as no significant delay with temperature variations initially from 386 °C, 409 °C and 426 °C, respectively. According to Eq. (11), for oxygen-saturated LBE, the EMF decreases with increasing temperatures, and EMF results of both sensors accorded with the trend.

Figure 7(b) shows the temperature fluctuation with the peaks as the inertia of heating cell of the experimental tank, but stayed at about 409 °C, 426 °C, and 443 °C, respectively. From Fig. 7(a) only at the first peak of each heating stage the EMF values of both sensors declined clearly, and small disturbance of temperature in a relatively short time did not change the oxygen concentration of LBE timely. Comparing the time consumed for initial response of the sensors at the three heating stages, faster responses of the sensors can be seen at higher start temperatures.

IV. CONCLUSION

Two Pt/air reference electrode oxygen sensors (Sensor 1, self-developed; and Sensor 2, from KIT) were tested in stagnant oxygen-saturated liquid LBE. Performances of the sensors are summarized as follows:

(a) In the calibration test, the corrected EMF data of Sensor 1 with 20 mV bias voltage showed consistent with theoretical results and the EMF data of Sensor 2, at temperatures above 425 °C. The calculated oxygen contents confirmed the above points.

(b) In stability test, Sensor 2 performed nicely, and the corrected EMF value of Sensor 1 was in accord with the theoretical one at 450 °C, though its signal fluctuations were a little large.

(c) In the responsiveness test, both sensors exhibited quick response to temperature variations, and faster response of the sensors was observed at higher start temperatures.

The results showed that Sensor 1 was suitable to measure dissolved oxygen concentration in LBE above 425 °C. How to reduce the signal fluctuation in long-term service and study the response performance are important issues to be addressed in the future work. The primary LBE charge/drain operation and circulation in KYLIN-II loop was succeed recently, and the test of self-developed Pt/air reference oxygen sensors in this loop is in progress.

ACKNOWLEDGEMENTS

The authors thank Dr. JIANG Zhi-Zhong of the FDS team and Mr. HE Long-Hai of Anhui Institute of Optics and Fine Mechanics, CAS, for useful discussions.

[1] Schroer C, Konys J, Verdaguer A, *et al*. J Nucl Mater, 2011, **415**: 338–347.
[2] Schroer C, Wedemeyer O, Konys J. Nucl Eng Des, 2011, **241**: 1310–1318.
[3] Courouau J L, Trabuc P, Laplanche G, *et al*. J Nucl Mater, 2002, **301**: 53–59.
[4] Rivai A K, Kumagai T, Takahashi M. Prog Nucl Energ, 2008, **50**: 575–581.
[5] Zhang J S and Li N. J Nucl Mater, 2008, **373**: 351–377.
[6] OECD. Handbook on lead-bismuth eutectic alloy and lead properties, materials compatibility, thermal hydraulics and technologies, 2007.
[7] Arkundato A, Su'ud Z, Abdullah M, *et al*. Ann Nucl Energy, 2013, **62**: 298–306.
[8] Kurata Y, Abe Y, Futakawa M, *et al*. J Nucl Mater, 2010, **398**: 165–171.
[9] Gabriele F D. Protocol and standards for HLM technology elements testing. FP7-249677-HeLiMnet, 2012.
[10] Shmatko B A and Rusanov A E. Mater Sci+, 2000, **36**: 689–700.
[11] Konys J, Muscher H, Voss Z, *et al*. J Nucl Mater, 2004, **335**: 249–253.
[12] Courouau J L. J Nucl Mater, 2004, **335**: 254–259.
[13] Courouau J L, Deloffre P, Adriano R. J Phys IV, 2002, **12**: 141–153.
[14] Wu X L. Master Thesis, University of Nevada, Las Vegas, 2004.
[15] Wu Y C, Huang Q Y, Zhu Z Q, *et al*. Chin J Nucl Sci Eng, 2009, **29**: 161–169. (in Chinese)
[16] Wu Y C and FDS Team. Nucl Fusion, 2007, **47**: 1533–1539.
[17] Wu Y C and FDS Team. Fusion Eng Des, 2007, **82**: 1893–1903.
[18] Wu Y C and FDS Team. J Nucl Mater, 2007, **367**: 1410–1415.
[19] Gao S, Zhang M L, Zhu Z Q, *et al*. Chin J Nucl Sci Eng, 2007, **27**: 51–54. (in Chinese)
[20] Huang Q Y, Gao S, Zhu Z Q, *et al*. Fusion Eng Des, 2009, **84**: 242–246.
[21] Huang Q Y, Li C J, Li Y F, *et al*. At Energ Sci Technol, 2007, **41**: 397–406. (in Chinese)
[22] Zhu L L, Bai Y Q, Chen Z, *et al*. Chin J Nucl Sci Eng, 2010, **30**: 333–337. (in Chinese)
[23] Wu Y C, Huang Q Y, Bai Y Q, *et al*. Chin J Nucl Sci Eng, 2010, **33**: 238–243. (in Chinese)
[24] Wang G Y, Bai Y Q, Gao S, *et al*. Chin J Nucl Sci Eng, 2012, **32**: 165–169. (in Chinese)
[25] Foletti C, Gessi A, Benamati G. J Nucl Mater, 2008, **376**: 386–391.
[26] Ghetta V, Fouletier J, Henault M, *et al*. J Phys IV, 2002, **12**: 123–140.
[27] Muscher H, Konys J, Voss Z, *et al*. Measurement of oxygen activities in eutectic lead-bismuth by means of the EMF method, FZKA 6690, 2001.
[28] Schroer C and Konys J. Physical chemistry of corrosion and oxygen control in liquid lead and lead–bismuth eutectic. FZKA 7364, 2007.
[29] Colominas S and Abella J. Sensor Actuat B-Chem, 2010, **145**: 720–725.
[30] Li N. J Nucl Mater, 2002, **300**: 73–81.
[31] Schroer C, Wedemeyer O, Konys J. Nucl Eng Des, 2011, **241**: 4913–4923.